South African seismicity, April 1997 to April 1999, and regional variations in the crust and uppermost mantle of the Kaapvaal craton

C. Wright[a,*], E.M. Kgaswane[a,1], M.T.O. Kwadiba[a,b], R.E. Simon[a,c], T.K. Nguuri[a,2], R. McRae-Samuel[a]

[a] *Bernard Price Institute of Geophysical Research, University of the Witwatersrand, Johannesburg, Private Bag 3, Wits 2050, South Africa*
[b] *Department of Geological Survey, Private Bag 14, Lobatse, Botswana*
[c] *Department of Physics, University of Botswana, Private Bag UB704, Gaborone, Botswana*

Abstract

Events induced by deep gold-mining activity on the edge of the Witwatersrand basin dominate the seismicity of South Africa. The deployment of 54 broad-band seismic stations at 84 separate locations across southern Africa between April 1997 and April 1999 (Kaapvaal network) enabled the seismicity of South Africa to be better defined over a 2-year period. Seismic events located by the South African national network, and by localized seismic networks deployed in mines or across gold-mining areas, were used to evaluate earthquake location procedures and to show that the Kaapvaal network locates mining-induced tremors with an average error of 1.56 ± 0.10 km compared with 9.50 ± 0.36 km for the South African network. Travel times of seismic events from the mines recorded at the Kaapvaal network indicate regional variations in the thickness of the crust but no clearly resolved variations in seismic wavespeeds in the uppermost mantle. Greater average crustal thicknesses (48–50 km compared with 41–43 km) are observed in the northern parts of the Kaapvaal craton that were affected by the Bushveld magmatism at 2.05 Ga. Estimates of average crustal thickness for the southern part of the Kaapvaal craton from receiver functions (38 km) agree well with those from refracted arrivals from mining-induced earthquakes if the crustal thicknesses below the sources are assumed to be 40–43 km. In contrast, the average crustal thickness inferred from refracted arrivals for the northern part of the Kaapvaal craton is larger by about 7 km (51 km) than that inferred from receiver functions (44 km), suggesting a thick mafic lower crust of variable seismic properties due to variations in composition and metamorphic grade. Pn wavespeeds are high (8.3–8.4 km/s), indicating the presence of highly depleted magnesium-rich peridotite throughout the uppermost mantle of the craton. Seismic Pg and Sg phases indicate that the upper crust around the Witwatersrand basin is comparatively uniform in composition when averaged over several kilometres.

Keywords: Crustal thickness; Kaapvaal craton; Mining-induced earthquakes; Composition of crust; Composition of uppermost mantle

1. Introduction

The Archaean Kaapvaal craton and adjacent Proterozoic mobile belts cover much of southern Africa (Fig. 1). Natural seismicity of southern Africa (Fig. 2)

* Corresponding author. Fax: +27-11-717-6579.
E-mail address: wrighto@geosciences.wits.ac.za (C. Wright).
[1] Present address: Council for Geoscience, Private Bag X112, Pretoria 0001, South Africa.
[2] Present address: PREPCOMM CTBTO, Vienna International Centre, PO Box 1250, A-1400, Vienna, Austria.

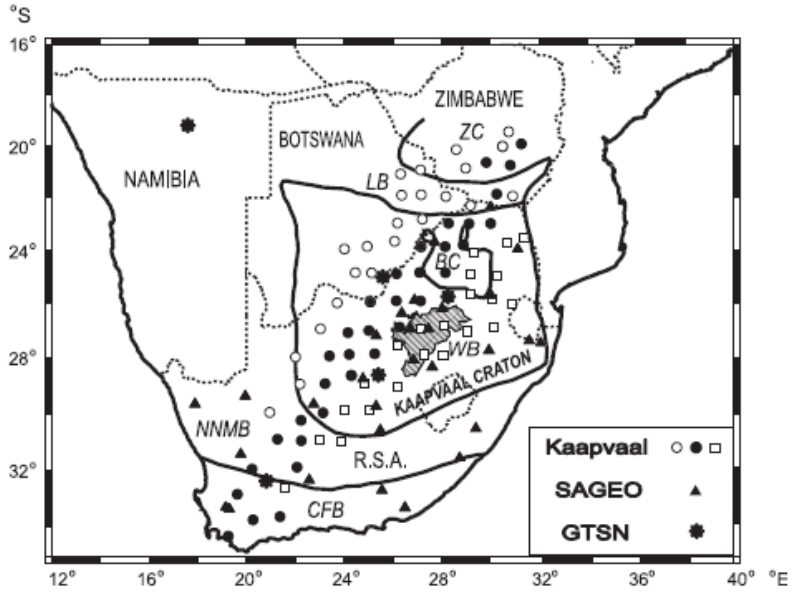

Fig. 1. Map of southern Africa showing distribution of seismic stations and main tectonic elements. BC = Outer boundary of surface outcrops of Bushveld complex; CFB = Cape Fold belt; LB = Limpopo belt; NNMB = Namaqua–Natal mobile belt; WB = Witwatersrand basin; ZC = Zimbabwe craton. Open and closed circles and squares denote stations of Kaapvaal broad-band network that operated from April 1997 to April 1998, April 1997 to April 1999 and April 1998 to April 1999, respectively. Triangles denote stations of South African network, and asterisks indicate broad-band stations of the Global Telemetered Seismic Network, or long-period stations.

is fairly typical of stable continental regions, with some areas of pronounced neotectonic activity (Andreoli et al., 1996), and with a largest instrumentally determined earthquake magnitude within South Africa of 6.3 (Green and Bloch, 1971). Almost a century ago, however, Wood (1913) reported that there was considerable seismicity in the Johannesburg area resulting from gold mining on the margin of the Witwatersrand basin. Such seismicity has persisted until the present day and, as mining operations move to greater depths, continues to pose a significant safety hazard to workers; it is monitored by networks of seismic instruments deployed in individual mines or distributed across particular goldfields (Mendecki, 1997).

A feasibility study on the use of mine tremors in South Africa for determining crustal structure was pioneered more than 50 years ago by Gane et al. (1946). P and S waves from these mining-induced events were subsequently used to determine the wave-speed structure of the crust and uppermost mantle around the Witwatersrand basin (Willmore et al., 1952; Gane et al., 1956; Hales and Sacks, 1959; Durrheim and Green, 1992; Durrheim, 1998a). However, only recently have such events been used in conjunction with local and regional tectonic events to determine earth structure from the surface to depths of 320 km (Wright et al., 2002).

There have been few seismological studies of earth structure within southern Africa compared with many other areas of the world such as Australia, North America and western Europe, so that there is a need to define regional travel time curves and the structure of the crust and upper mantle to better understand cratonic evolution and to enable earthquakes to be more accurately located.

Between April 1997 and April 1999, a network of 54 broad-band seismic instruments was deployed at 84 different locations across southern Africa (Carlson et al., 1996) as part of the international Kaapvaal

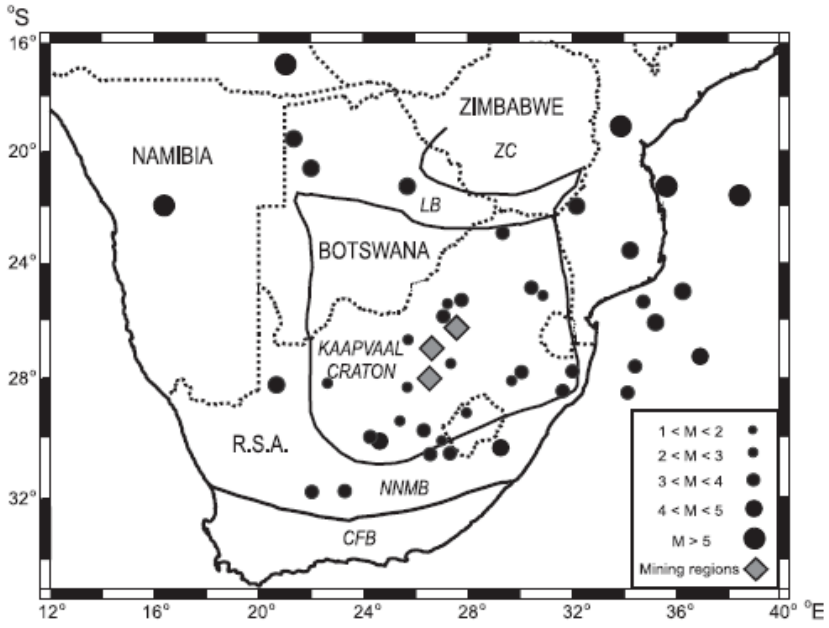

Fig. 2. Seismicity of southern African region, April 1997 to April 1999, showing tectonic events located by the Council for Geoscience. CFB, LB, NNMB and ZC are described in the caption to Fig. 1. The most seismically active areas of gold mining are, from north to south: Far West and West Rand, Klerksdorp and Welkom.

craton program (Fig. 1). The main objective of this seismic experiment was to derive tomographic images of the crust and mantle to depths of about 700 km using recordings of teleseismic earthquakes (i.e., earthquakes at distances greater than 3300 km). However, the network also recorded local (distances less than 300 km) and regional earthquakes (distances between 300 and 3300 km), thus enabling more detailed information on the seismicity of southern Africa to be obtained over a 25-month period.

The purpose of the present work is to show how a temporary network of three-component, broad-band seismometers deployed across southern Africa supplements the South African National seismic network in defining seismicity and in improving the accuracy of the determination of catalogued seismic events. The temporary network is then used to define average P and S travel time curves and wavespeed models for the southern African region to improve earthquake locations. Locations of mining-induced earthquakes from mine seismic networks provide a large number of seismic events distributed over five distinct mining regions that are sufficiently accurate to be regarded as equivalent to explosive sources used in crustal refraction studies in other parts of the world. Regional differences in the structure of the crust and uppermost mantle of the Kaapvaal craton are then defined through analysis of the seismograms of these mining-induced events. These differences are interpreted with information from receiver functions to provide constraints on deep-seated petrological variations.

2. Sources of information on earthquakes

Information on the locations and magnitudes of earthquakes within South Africa, neighbouring countries and adjacent oceanic regions, for the period April 1997 to April 1999, comes from bulletins

published by the Council for Geoscience, which is derived from seismograms recorded by the short-period seismometers of the South African network (Graham, 1997, 1998, 1999). Magnitudes are from 1.0 for some mining-induced events upwards. Locations of most events of local magnitude greater than 4 are also listed in preliminary earthquake bulletins issued by the United States Geological Survey.

The South African seismic network locates events using a limited number of stations (typically 4–8), so that epicentres are not expected to be particularly accurate. The large number of three-component seismic stations deployed across southern Africa as part of the international Kaapvaal experiment enables relocation of the larger seismic events (magnitudes >2.5) with more data, and with a new regional reference model and travel times (Simon et al., 2002; Wright et al., 2002). To compare earthquake locations made by the South African and Kaapvaal networks, accurate locations of events by some other means is required. Seismic networks operated by the mining industry across mining regions or within individual mines locate far more events than are published in the Council for Geoscience Bulletins (Graham, 1997, 1998, 1999), and for which the location errors in most cases are less than 400 m (Webb et al., 2001). Catalogues of earthquakes prepared by the mining industry can therefore be used to evaluate the relative location accuracies of mining-induced events by the South African and Kaapvaal networks, for which the location errors are expected to be greater than a kilometre. The resulting estimates of location errors will then give insight into the errors in locating tectonic earthquakes away from the mining areas, which will be used in future for studying earth structure.

3. Correlations and database

The production of a comprehensive catalogue of seismic events for South Africa of magnitude greater than 2 for the period April 1997 to April 1999, and the development of a database of waveforms of events listed in the Council for Geoscience bulletins recorded by the Kaapvaal network, was required as the first stage in this work. The procedures used for correlating events reported in the Council for Geoscience bulletins with those appearing in catalogues prepared by the mining industry, and for reducing all locations to a common coordinate system of latitudes and longitudes were described by Webb et al. (2001) and Kgaswane (2002). A summary of these procedures, and some comments on the results are as follows.

The Council for Geoscience operated 29 seismic stations throughout South Africa (Fig. 1) that were used to produce earthquake bulletins (Graham, 1997, 1998, 1999) during the 25 months of operation of the Kaapvaal network. Catalogues of events from seven mines in the Far West Rand, two in the West Rand, one in the East Rand, and for the regional networks operated in the Klerksdorp and Welkom areas formed the input data (not complete) from the gold-mining areas, which are shown in Fig. 3. The steps in the analysis of the data, the search for common events in the Council for Geoscience and mine catalogues and the production of a database for future research were outlined by Kgaswane et al. (2002).

A total of 429 events common to both mine and Council for Geoscience catalogues was relocated using the program HYPOELLIPSE (Lahr, 1989), data from the Kaapvaal network, a local reference travel time curve for P that was used to derive earth model BPI1 of Wright et al. (2002) and a similar travel time curve for S whose derivation is discussed in Section 4. Assuming that errors in locations from mine catalogues could be neglected, the average errors in locations from the South African network and from the Kaapvaal network were 9.50 and 1.56 km, respectively (Kgaswane, 2002; Kgaswane et al., 2002).

Table 1 summarises the most important results from the catalogue correlations and relocations. Data from the mine catalogues were cut off below a moment magnitude of 1.7. The magnitude range of the 1578 correlated events is 1.7–4.5 from the mine catalogues and 1.4–5.1 for the local magnitudes of the Council bulletins (Graham, 1997, 1998, 1999). A combined total of 4414 events in the gold-mining regions was located with a minimum magnitude of 1.1 in the Council bulletins, and 1.7 in the mine catalogues. The largest event in the mine catalogues had a magnitude of 4.5, but the same event in the Council bulletins was given a magnitude of 5.1. The magnitudes from the mine catalogues are systematically lower at high magnitudes and similar or slightly higher at low magnitudes than those in the Council

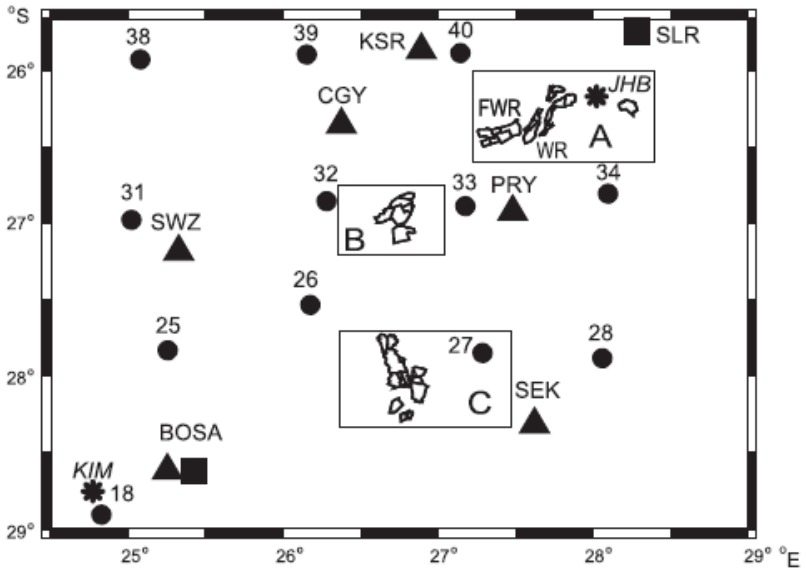

Fig. 3. Map of gold-mining areas on the margin of the Witwatersrand basin. (A) Far West Rand, West Rand and Central and East Rand from west to east. (B) Klerksdorp. (C) Welkom. KIM: Kimberley. FWR: Far West Rand. JHB: Johannesburg. WR: West Rand. Numbers and circles denote stations of the Kaapvaal network. Three- or four-letter codes and triangles denote stations of the South African network. Permanent broad-band or long-period stations are shown as squares.

bulletins, and the reasons for these differences were discussed by Kgaswane et al. (2002).

The catalogue of events summarised in Table 1 shows that over 4400 seismic events with mine magnitudes greater than 1.7 occurred during the period of the Kaapvaal experiment, of which over 4000 have been located with accuracies better than 400 m. Many of the smaller events of magnitudes less than 2.5 are located with errors less than 100 m. These events are all in the central region of the Kaapvaal craton. The merged catalogue is clearly incomplete, since separate catalogues were not available for many seismically active mines in the Far West Rand, West Rand and Central and East Rand regions. Furthermore, 16.5% of the events in mining regions that appeared in the Council catalogues were absent from the mine catalogues, including the regional networks for Klerksdorp and Welkom (8.9% and 33.5%, respectively). Thus, periods during which both the regional seismic networks and the networks in individual mines were not functioning also contribute to the lack of completeness of the merged catalogue. Only 42 tectonic events were located by the South African network during the period April 1997 to April 1999 (Fig. 2), of which 18 were outside South Africa (Webb et al., 2001), though many more tectonic events within southern Africa were recorded by the Kaapvaal network. These events are undergoing further analysis, so that they can be used for tomographic imaging of the crust and uppermost mantle of the region.

4. Reference travel time curves

Fig. 4(a) shows part of a reference P wave travel time curve plotted as reduced time to distances of 1200 km, derived from travel times of earthquakes within South Africa, adjacent countries and surrounding oceans. The time data from both the South African and Kaapvaal networks are superimposed and, at short distances, consist predominantly of times from events

Table 1
Summary of the most important results from the catalogue correlations and relocations for the period April 1997 to April 1999, inclusive

Region	No. of correlated events and magnitude range (mine)	No. of events in mine catalogues, but absent from Council bulletins, and magnitude range (mine)	No. of events in Council bulletins, but absent from mine catalogues, and magnitude range (Council)	Total events	Percentage of events in Council bulletins absent from mine catalogues
East and Central Rand[a]	6	27	63	96	91.3
	1.7–3.0	1.7–3.0	1.8–3.8		
Far West Rand	773	1849			
	2.0–4.1	1.8–3.4			
West Rand	159	105			
	2.0–3.4	2.0–3.1			
Far West Rand and West Rand[b]	932	1954	127	3013	12.0
	2.0–4.1	1.8–3.4	1.3–3.2		
Klerksdorp	503	433	49	985	8.9
	2.0–4.0	2.0–3.3	1.1–4.1		
Welkom	137	114	69	320	33.5
	2.0–4.5	2.0–2.9	2.0–3.8		
All regions	1578[c]	2528	308	4414	16.3
	1.4–5.1 (Council)	1.7–3.4	1.1–4.1		

[a] Mine catalogue for East Rand Proprietary Mine was available only from 24 August to 1 December 1998.
[b] For comparison with Council for Geoscience bulletins, the Far West Rand and West Rand regions were combined, because errors in Council locations make it impossible to separate uncorrelated events for these two closely spaced regions (Fig. 3).
[c] One event in Council for Geoscience bulletins corresponds to two events at the Elandsrand mine closely separated in space and time, so that there were only 1577 correlated events in the Council for Geoscience catalogues.

in gold-mining areas recorded at stations in and around the Witwatersrand basin. These data were derived before accurate locations of mining-induced events were available, so that the epicentres of all events within South Africa and surrounding countries and oceans were obtained from the Council for Geoscience earthquake bulletins (Graham, 1997, 1998, 1999), while epicentres of more distant events were taken from the United States Geological Survey Preliminary Determinations of Epicenters. The numerical and statistical methods used to derive the reference travel time curve were described by Wright et al. (2002). The most important features of the data are the 'hump' in the reduced travel time curve with a peak at a distance of 230 km, and the relatively large scatter of the data beyond distances of 200 km, where the expected first arrivals have paths through rocks with upper mantle wavespeeds.

Fig. 5 shows two average P wavespeed models to depths of 180 km that fit the data according to different criteria (Wright et al., 2002). The first model BPI1 was chosen as the simplest, using the criterion that the wavespeed gradients must be positive throughout the mantle. The peak in the reduced travel time curve at a distance of 230 km (Fig. 4(a)) was assumed to result from failure to identify the Pn arrivals at distances between about 170 and 240 km. Beyond 240 km distance, the Pn signals were believed to become larger, so that the Pn arrival was picked more frequently, thus pulling the smooth curve down towards the time at which it should be observed, merging with the expected times at distances near 400 km. The difficulty with model BPI1 is that it gives an average crustal thickness of 34 km, which is systematically lower by about 6 km than the average over the same region estimated from the receiver functions of Nguuri et al. (2001), but is in satisfactory agreement with crustal thicknesses estimated by earlier workers using mining-induced events (Willmore et al., 1952; Gane et al., 1956; Hales and Sacks, 1959; Durrheim and Green, 1992). Model BPI2 (Fig. 5) was constructed in an attempt to reconcile the differences in the average thickness of the crust estimated from refracted arrivals and from receiver functions, and to

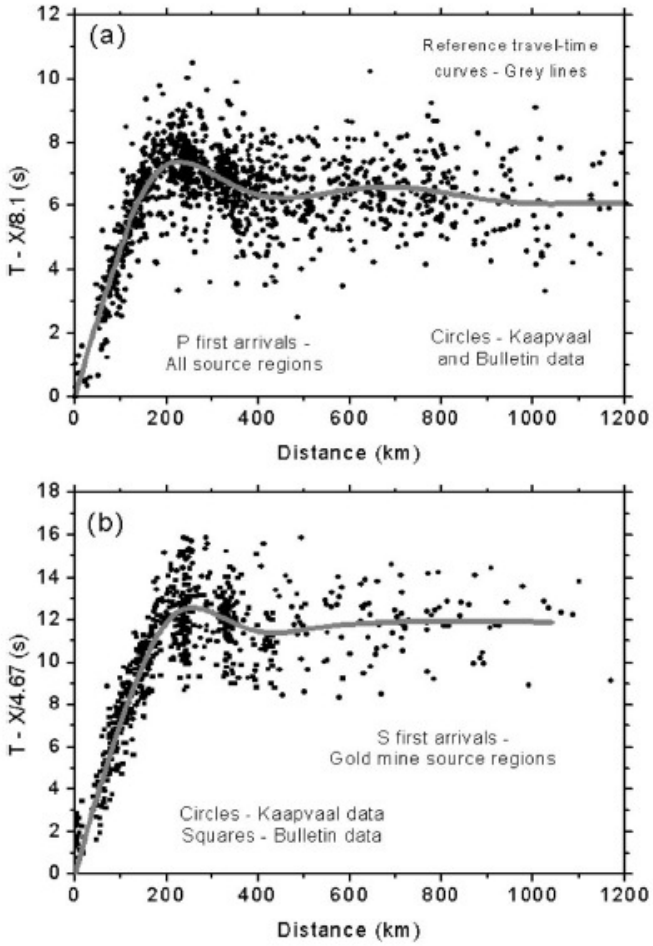

Fig. 4. (a) Reference P wave travel time curve for the southern African region plotted as reduced times to a distance of 1200 km, together with the data from which it was derived. (b) Corresponding S wave travel time curve for the southern African region plotted as reduced time, together with the data from which it was derived.

explain some of the anomalous features of the travel times (Wright et al., 2002). It has a region of seismic wavespeeds of about 8.0 km/s between depths of 36 and 47 km, whose petrological nature (crust or mantle?) remains uncertain, with a relatively high wavespeed of 8.23 km/s at depths between 47 and 65 km. A low wavespeed zone between depths of about 65 and 125 km with an average wavespeed of 8.1 km/s is then required to prevent the travel times computed from the model from becoming too early at distances greater than 1000 km. Since the most of the seismic sources are concentrated in the gold-mining areas of the central part of the Kaapvaal craton, it is not clear if the requirement for a low wavespeed zone in the one-dimensional model BPI2 (Fig. 5) arises from lateral variations in structure as the margins of

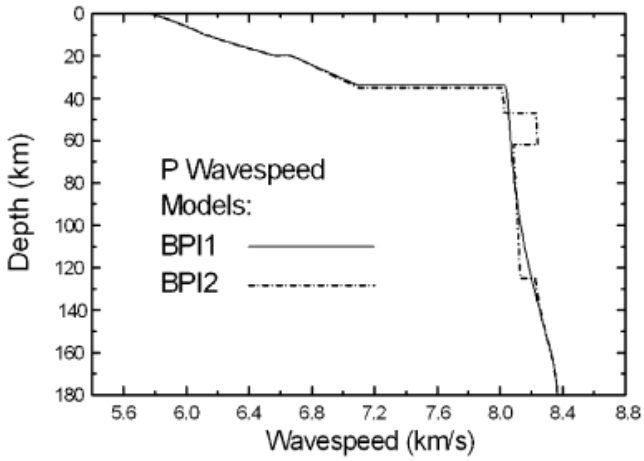

Fig. 5. P wavespeed models BPI1 and BPI2 to a depth of 180 km.

the cratonic nucleus are sampled by the stations that are more distant from the sources.

Fig. 4(b) shows the reduced travel times to distances of 1200 km and calculated smooth curve to distances of 1040 km for the earliest S wave arrivals, which also show the prominent peak near 230 km distance that was clearly resolved for P waves. The input data consist of 506 times from 105 mining-induced events listed in the Council for Geoscience earthquake bulletins (Graham, 1997, 1998, 1999) for earthquakes in the gold-mining regions. Bulletin data for both P and S were included to better constrain the seismic wavespeeds in the crust, since the data at short distances from the Kaapvaal network are relatively sparse. The remaining S wave data consist of times from eight accurately located mining-induced events (see Section 5). The times were corrected for origin time errors in a similar manner to the P wave data (Wright et al., 2002).

A smooth curve was then fitted through the combined first arrival times (Sg and Sn) times to distances of 1000 km (Fig. 4(b)) by the method of summary values (Jeffreys, 1937; Bolt, 1978). A cubic smoothing spline was then fitted through the summary points using the algorithm of Reinsch (1967) to give both a reference S wave travel time curve and a slowness curve that was used to derive a wavespeed model to depths of 40 km by Herglotz–Wiechert inversion (Shearer, 1999, pp. 66–67). When this method of analysis was used on the P wave data, the result was virtually indistinguishable from the 14th degree polynomial shown in Fig. 4(a) (Simon et al., 2002), showing that the result is not dependent on the method of curve fitting.

Table 2
Average P and S wavespeed models of the crust for the Kaapvaal region and uppermost mantle (BPI1) for southern Africa[a]

Depth (km)	S wavespeed (km/s)	P wavespeed (km/s) (range)	Poisson's ratio
0	3.462	5.594–5.927	0.190–0.241
5.0	3.553	5.903–6.133	0.216–0.247
10.0	3.659	6.133–6.286	0.224–0.244
15.0	3.752	6.385–6.454	0.236–0.245
20.0	3.806	6.591	0.250
20.0	3.926	6.800	0.250
27.0	3.954	6.950	0.261
34.0	3.982	7.100	0.271
34.0	4.639	8.035	0.250
40.0	4.647	8.049	0.250
50.0	4.653	8.059	0.250
60.0	4.658	8.067	0.250

[a] The P wavespeeds listed are a small modification of model BPI1 called BPI1A, due to the addition of two events and construction of a new model (Simon et al., 2002).

The smooth model was then modified by comparison with the equivalently derived smooth P wavespeed model, to give the shear-wave equivalent to model BPI1 of Wright et al. (2002) with discontinuities at depths of 20 and 34 km (Table 2). This model has an increase in Poisson's ratio from 0.19 at the surface to 0.27 at the crust–mantle boundary. The fitting of an average S model for the upper mantle is subject to the same problems encountered for P due an increase in slowness with increasing distance (Fig. 4). The average model for S (BPI1) is not shown here, but it is incorporated into the work of Simon et al. (2003). The average models for P and S at mantle depths are for the southern African region, and therefore represent a weighted average for the Kaapvaal craton and surrounding mobile belts. The next step is to focus on resolving regional differences in seismic structure with emphasis on the Kaapvaal craton.

5. Regional P and S wave times across southern Africa

Earliest P arrival times from 20 accurately located mining-induced events for each of regions A, B and C of Fig. 3 were picked from seismograms bandpass-filtered between 0.4 and 4.0 Hz, and the data for region A are shown in Fig. 6. The data for each source region were divided into two groups according to source–receiver paths: those corresponding to paths predominantly through the undisturbed southern part of the Kaapvaal craton and the Namaqua–Natal and Cape Fold belts (Fig. 7), and those with paths through the northern regions in which the original Archaean lower crust and possibly the uppermost mantle may have been altered by the Bushveld event at 2.05 Ga (Nguuri et al., 2001). Times are significantly longer for the northern stations to distances of about 650 km but become closer to those for southern stations at larger distances. The data to the south show an offset or upward curvature at distances greater than 650 km. Wright et al. (2002) suggested that this effect could be produced by a low wavespeed layer in the upper mantle at depths between 65 and 125 km. An alternative explanation is a significant decrease in seismic wavespeeds in the upper mantle across the southern margin of the Kaapvaal craton.

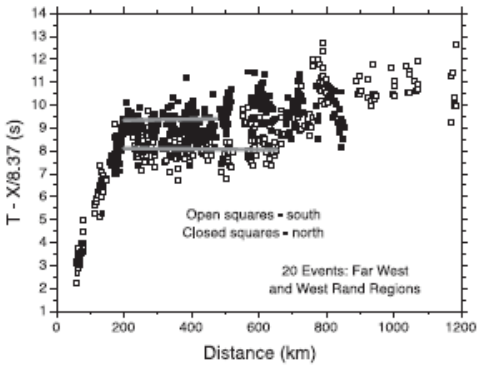

Fig. 6. Reduced travel times for P wave first arrivals for 20 accurately located mining-induced earthquakes in the Far West and West Rand regions (Fig. 3). Regression lines through the Pn arrivals at stations in the northern and southern areas of the craton (Fig. 7) are the upper and lower lines, respectively.

Regression lines have been fitted through the Pn times from the northern and southern regions for distances beyond 200 km for stations that lie within the Kaapvaal craton, and the results are shown in Table 3. From the slopes of these lines, the estimated average seismic wavespeeds in the uppermost mantle for the three separate source regions are in the range 8.33–8.43 and 8.30–8.32 km/s for the northern and southern regions, respectively, suggesting only minor differences in mantle wavespeeds between the southern region and the northern region that includes the Bushveld complex.

Average P wavespeed models for the northern and southern parts of the craton were derived from the data of Fig. 6 by ray tracing for a spherical earth. No attempt was made to revise the P wavespeeds in the crust, the values from BPI1A (Table 3; Simon et al., 2002) being used. There is at present no clear evidence for differences in wavespeeds in the upper crust for different parts of the craton, and wavespeeds in the lower crust are not well resolved. The thickness of the crust was varied between 34 and 52 km, keeping the wavespeeds at 20 km depth and at the crust–mantle boundary constant at 6.80 and 7.10 km/s with a constant wavespeed gradient between these depths. Upper mantle wavespeeds with low wavespeed gradients below the crust–mantle transition, but with average values close to 8.33 and 8.31 km/s were used

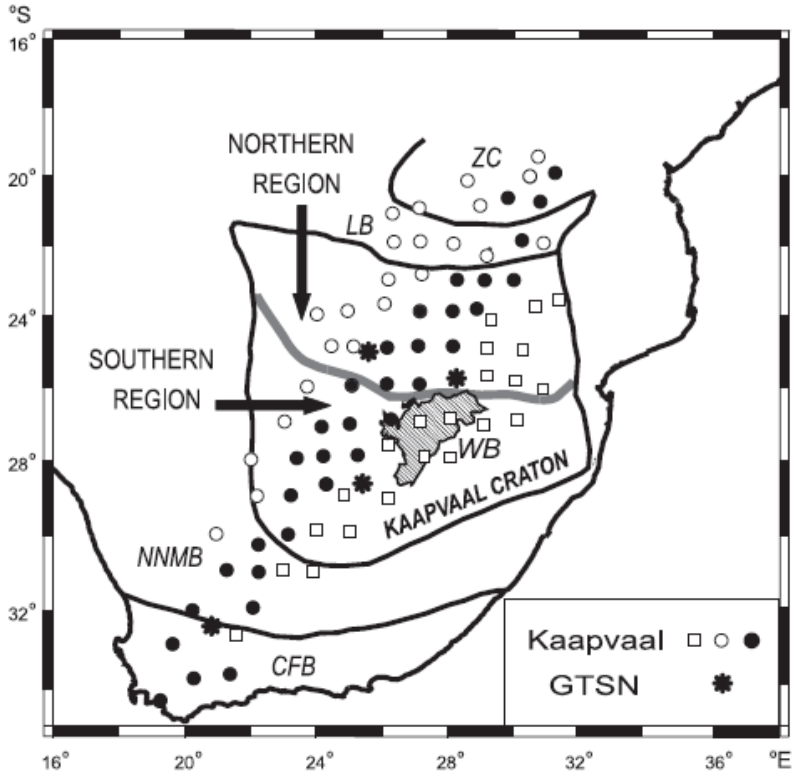

Fig. 7. Map showing division of source–station paths into northern and southern regions. Circles, squares, asterisks and two- to four-letter abbreviations have the same meaning as in Fig. 1.

for the northern and southern regions, respectively. The best model fits to the data are shown in Fig. 8 for events for the Far West and West Rand regions and were chosen to be those that produced a good fit to the regression lines of Table 3. Reduced travel time curves are shown for the best fitting models and for

Table 3
Regression lines of form $T=a+bx$ for Pn and Sn for southern and northern regions of the Kaapvaal craton

Description	a (s)	b^{-1} (km/s)	Distance range (km)	S.D. on residuals (s)	No. of observations	V (km/s, corrected for curvature of Earth)
P North FWR	9.293 ± 0.15	8.386 ± 0.032	205–474	0.48	205	8.333 ± 0.032
P North KLE	9.182 ± 0.12	8.468 ± 0.027	228–553	0.47	204	8.415 ± 0.022
P North WEL	9.498 ± 0.15	8.485 ± 0.022	340–648	0.47	208	8.432 ± 0.022
P South FWR	8.143 ± 0.12	8.360 ± 0.020	228–652	0.46	249	8.308 ± 0.020
P South KLE	7.659 ± 0.16	8.357 ± 0.029	200–555	0.65	209	8.305 ± 0.029
P South WEL	7.997 ± 0.16	8.365 ± 0.032	201–488	0.65	262	8.313 ± 0.032
S North (all)	16.148 ± 0.48	4.826 ± 0.030	211–648	1.12	50	4.796 ± 0.030
S South (all)	14.343 ± 0.57	4.857 ± 0.035	200–646	1.41	58	4.827 ± 0.035

FWR, KLW and WEL denote the Far West and West Rand, Klerksdorp and Welkom mining regions, respectively.

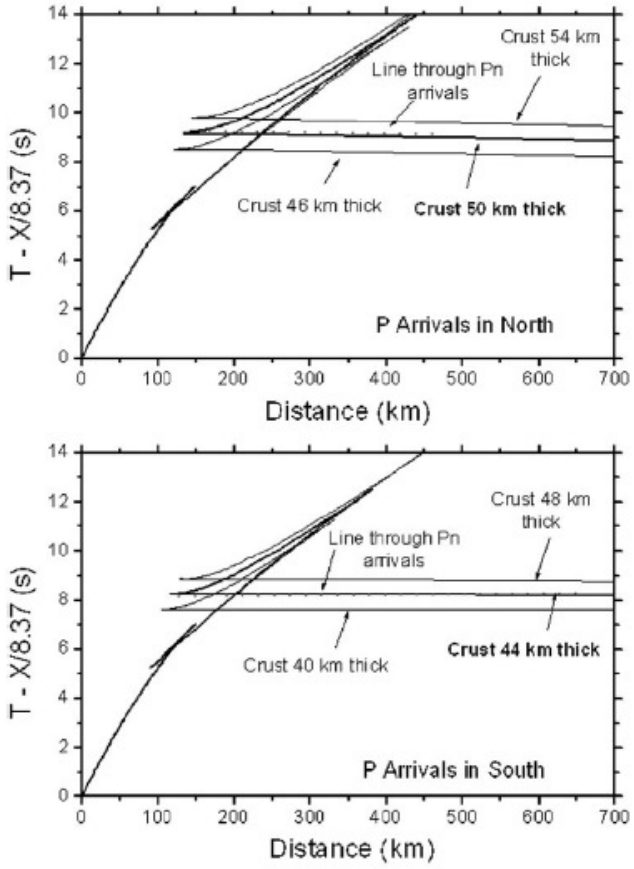

Fig. 8. Average P wavespeed models for the northern (top) and southern (bottom) regions of the Kaapvaal craton, derived from 20 mine tremors in the Far West and West Rand regions.

models with crustal thicknesses 4 km thicker and thinner. The average crustal thicknesses in the northern and southern regions are 50 and 44 km, respectively, with an estimated precision of about 1 km in each case.

Table 4 shows the separate results for the three main source regions, indicating a mean thickness for paths from the Witwatersrand basin to the northern and southern parts of the craton (Fig. 7) of about 50 and 42–43 km, respectively. These thicknesses are strongly weighted by the thicknesses in the source regions, and they tend to be larger than those estimated from receiver functions, especially for the northern part of the craton (Kwadiba et al., 2003). Using estimates of crustal thicknesses at each station, assuming the same thickness at each source region, there is a systematic difference of 2.5 ± 0.30 km (34 stations) and 2.2 ± 0.35 km (31 stations), respectively, between results from the West Rand and Klerksdorp and from the West Rand and Welkom source regions. This establishes that the crustal thicknesses are 2.5 and 2.2 km less below the Klerksdorp and Welkom regions, respectively, than beneath the Far West and West Rand (Kwadiba et al., 2003).

Table 4
Average crustal thicknesses in the northern and southern regions of the Kaapvaal craton estimated from refracted P and S arrivals

Source region and wave type	Thickness (km, North)	Minimum thickness (km, North)	Thickness (km, South)	Minimum thickness (km, South)	No. of events used	Pg–Pn cross-over distance (km)[a]
Far West and West Rand, Pn	50	48	44	42	20	207 N, 181 S
Klerksdorp, Pn	49	47	41	39	20	198 N, 169 S
Welkom, Pn	51	49	42	40	20	205 N, 176 S
All regions, Sn	52	–	44	–	8	216 N, 188 S

[a] The cross-over distances were estimated from the Pg, Sg, Pn and Sn times used in this paper. However, the cross-over distances in Figs. 8 and 10 are at larger distances. The reason is that the travel time curves in these figures correspond to the models of Table 2, which were derived from events for which accurate locations were not available, and for which it was not possible to reliably separate Pg and Pn or Sg and Sn arrivals at distances between about 170 and 220 km. The estimates of crustal thickness are not seriously biased by this effect, since it is the average wavespeed within the crust that controls the crustal thicknesses. Nevertheless, the need to refine the models of Table 2 using only data from accurately located mining tremors is recognized.

Fig. 9 shows the same data for S waves as Fig. 4(b), with the bulletin data removed, and with different symbols for the northern and southern regions. All seismograms were rotated to give radial and transverse components, and S times were picked from both sets of rotated seismograms to give travel times of SV (vertically polarised shear waves) and SH (horizontally polarised shear waves), respectively. Seismograms were bandpass-filtered between 0.2 and 2.0 Hz prior to picking times, noting that a lower frequency band than for P was required to maximize the clarity of the S arrivals. Since there is no clear evidence for any systematic differences between times

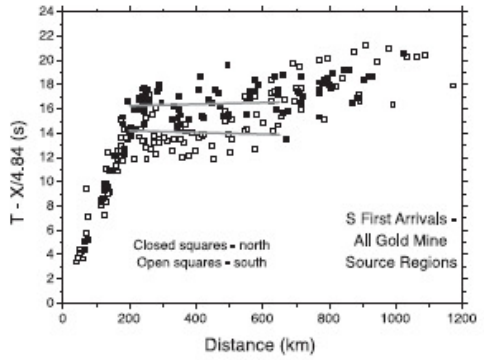

Fig. 9. Reduced travel times for S wave first arrivals for accurately located mining-induced earthquakes divided into two regions: stations in the southern part of the Kaapvaal craton, and in the northern part of the Kaapvaal craton overlying deep crust and uppermost mantle influenced by the Bushveld magmatism (Fig. 7). The upper and lower regression lines are fitted through the northern and southern Sn arrivals, respectively.

for SV and SH waves that might indicate shear-wave splitting, the times shown are the average of the SV and SH time picks.

As for P, times are significantly longer for the northern stations to distances of about 650 km, but they become closer to those for southern stations at longer distances. The properties of the S data for the northern and southern regions are generally similar to those of P, though the scatter is greater. Separate regression lines were fitted through the times measured at stations in the northern and southern parts of the Kaapvaal craton (Fig. 7) for distances greater than 200 km, and the results are listed in Table 3. From the slopes of these lines, approximate seismic wavespeeds in the uppermost mantle for the northern and southern regions are not significantly different, and are 4.796 ± 0.030 and 4.827 ± 0.035 km/s, respectively.

Average S wavespeed models for the northern and southern parts of the craton (Fig. 10) were derived from the data of Fig. 9 in exactly the same way as the P wave models of Fig. 6. Reduced travel time curves are shown for the best fitting models and for models with crustal thicknesses 4 km thicker and thinner. The estimated average crustal thicknesses in the northern and southern regions are 52 and 44 km, respectively, with an estimated precision of about 2 km in each case and are slightly higher than the values derived from P waves (Table 4).

6. Accuracy of origin times

Since the average crustal thicknesses imply values at individual stations greater than those from receiver

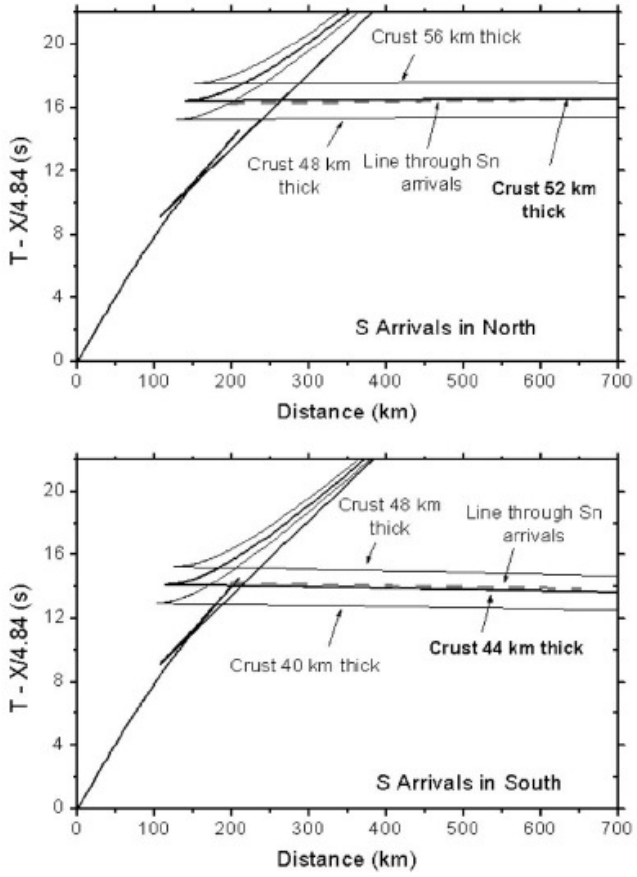

Fig. 10. Average S wavespeed models for the northern (top) and southern (bottom) regions of the Kaapvaal craton, derived from mine tremors in the Far West and West Rand (3), Klerksdorp (3) and Welkom (2) regions.

functions (see Section 8), we must determine if there is any bias in origin times that might affect the estimates of crustal thicknesses from refracted arrivals. The origin times provided in earthquake bulletins were corrected by reference to a travel time curve derived from times of P arrivals (Pg phase) at stations of both the South African and Kaapvaal networks (Simon et al., 2002; Wright et al., 2002). The model derived from the travel time curve (Table 2) does have relatively low near-surface wavespeeds, which could result from inaccurate and biased epicentre locations at short distances. The average wavespeeds of near-surface rocks in the Witwatersrand basin area could be as high as 6.0 km/s if crack porosity is low (e.g., Green and Chetty, 1990). The estimates of crustal thicknesses have been computed again using the higher P wavespeeds of Table 3, which provide a 'maximum wavespeed' model (Fig. 11); it yields a P travel time curve that produces an average forward shift in origin times of 0.46 s. The result is faster times for Pg and Pn than before, but the effect on Pg is greater than for Pn. The consequence is that all

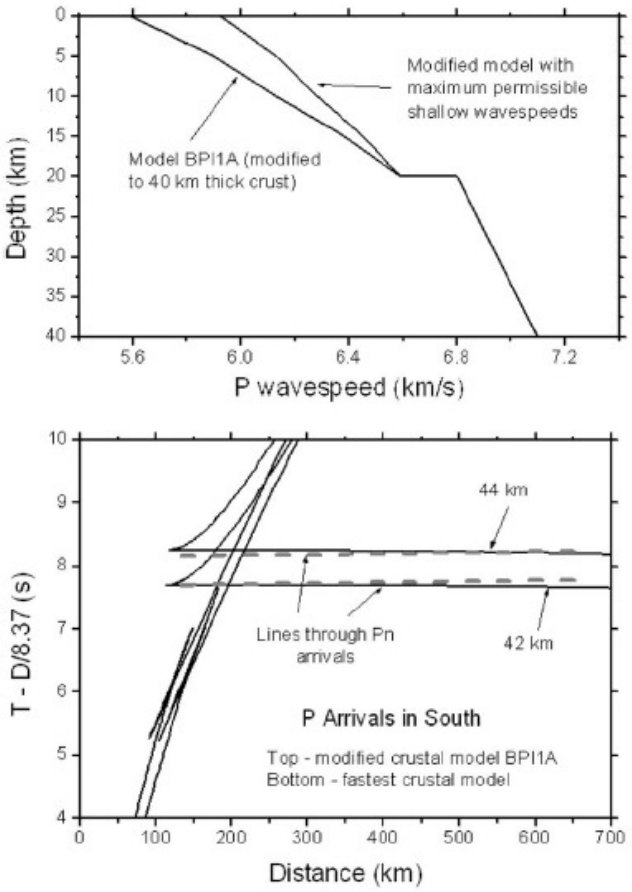

Fig. 11. Top: P wavespeed model BPI1A and modified model with 'maximum possible' wavespeeds in the upper crust. Moho is at 40 km depth. Bottom: Reduced travel times for 'best fit' models through data, using both wavespeed models shown above.

estimates of crustal thickness are reduced by 2 km (Fig. 11 and Table 4), which can be regarded as 'minimum thicknesses'.

A check on the suitability of the P reference travel time curve was obtained using the S travel times, since they were all corrected using data from P arrivals. The S times of Figs. 4b and 9 provide travel time curves that yield acceptable wavespeeds at shallow depths (Table 5). Furthermore, reducing the travel times at short distances by 0.46 s, results in a slight increase in slope with increasing distance to get zero time at zero offset, suggesting that a revised correction of 0.46 s to origin times is too large. The S times thus confirm that use of times computed from the higher wavespeed model of Table 2 will yield minimum estimates of crustal thicknesses.

7. Regional seismic phases

At distances greater than about 200 km, the most commonly observed later phases (i.e., signals that

Table 5
Regression lines of form $T = a + bx$ for Pg and Sg for the Kaapvaal craton (distance ranges 0–200 and 200–670 km for P, and 0–200 and 200–1170 km for S)

Description	a (s)	b^{-1} (km/s, average V)	S.D. on residuals (s)	No. of observations
Pg (0–200 km)	0.683 ± 0.20	6.214 ± 0.054	0.46	52
Pg (200–670 km)	0.290 ± 0.53	6.178 ± 0.050	1.15	56
Sg (0–200 km)	-0.037 ± 0.45	3.544 ± 0.039	1.03	50
Sg (200–1170 km)	0.192 ± 0.30	3.634 ± 0.0071	1.67	236

arrive later than the earliest arrivals that traverse the mantle, Pn and Sn) are denoted Pg and Sg, which are waves that travel entirely within the upper and middle crust. They are observed in the southern African region to distances of about 700 and 1200 km, respectively (Fig. 12). Figs. 13 and 14 show specimen seismograms for P and S arrivals, respectively, for a mine tremor in the Klerksdorp area on 13 September 1997. Fig. 13 shows a clear Pn arrival followed by a large, clear Pg phase about 7 s later at a distance of 364.6 km recorded by a station south of the Limpopo belt in eastern Botswana. Later Pg phases of this clarity are relatively uncommon. Fig. 14 shows a weak Sn arrival at a distance of 661.3 km, identifiable only on the transverse component, followed by a strong Sg arrival some 26 s afterwards. The station is on the Zimbabwe craton, near the southwestern margin. It is easier to identify the Sg arrivals at distances greater than 200 km, which tend to have clearer onsets than the Pg phase, resulting in the larger number of Sg observations in Fig. 12.

The slopes of the Pg and Sg curves can be used to constrain P and S wavespeed models for the upper and middle crust, provided there are sufficient data. Table 5 shows the results of fitting two regression lines through the Pg and Sg times for the eight events used to determine the Sn wavespeeds: (i) at distances less than 200 km, where they are the earliest P or S arrivals, and (ii) at greater distances where they are later phases and the onsets less clearly defined. The scatter of the data at distances beyond 200 km is greater, as indicated by the standard deviations on the residuals to the linear fits. The results show that there is no clearly resolvable increase in wavespeed with increasing distance for Pg or Sg either as first arrivals or as later arrivals, though for Sg the average value of 3.634 ± 0.0071 km/s for the later arrivals between distances of 200 and 1170 km is significantly greater than the value of 3.544 ± 0.039 km/s for short distances. The data of Table 5 yield values of Poisson's ratios of 0.262 and 0.235 for short distances (<200 km) and long-distance observations of Pg and Sg, respectively. Unfortunately, the difference between these two estimates of Poisson's ratio for the upper crust is too large to enable much to be inferred about

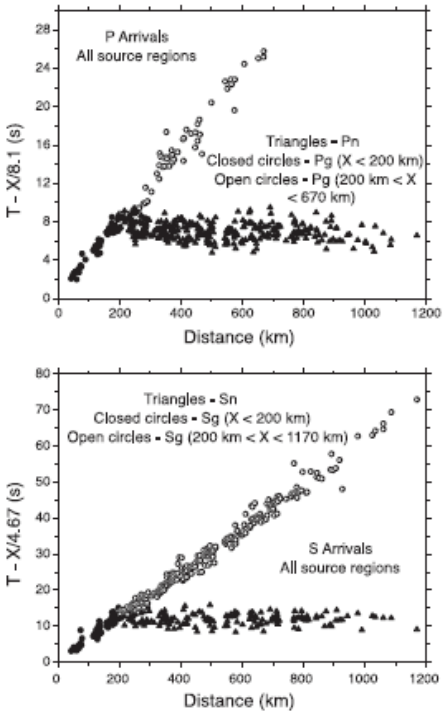

Fig. 12. Observations of the crustal phases, Pg and Sg, plotted as reduced travel times with Pn and Sn, for the eight events used in Fig. 9.

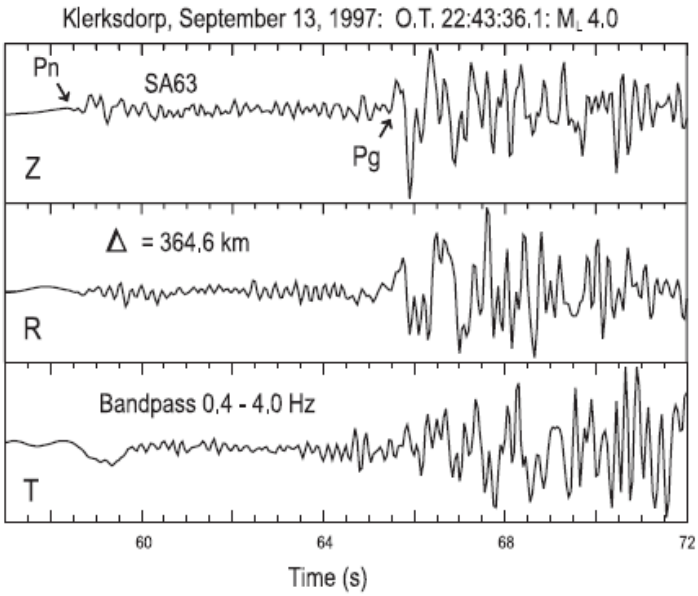

Fig. 13. Seismograms from a mine tremor at Klerksdorp on 13 September 1997 to illustrate observed P phases. Z, R and T denote vertical, radial and transverse components of motion, respectively. Zero of time scale is from the start of the file, and not from the origin time of the event.

the average composition. However, further work on a larger suite of Pg and Sg observations may assist in better defining the average structure and composition of the upper crust.

The mantle phases PmP and SmS (reflections from the crust–mantle boundary) generated by earthquakes are often large in amplitude but have emergent arrivals. Although, in principle, they can be used to estimate crustal thicknesses in continental regions, reliable estimates of such thicknesses are rare. An exception is the study of PmP and crustal thicknesses by Richards-Dinger and Shearer (1997). Several clear PmP phases were identified at distances beyond 110 km from mining-induced events by Kgaswane (2002), but due to emergent onsets, more work will be required to get reliable estimates of crustal thicknesses from them. A clear suite of PmP arrivals at one station from an array of sources in the Klerksdorp region yielded a crustal thickness of 40–42 km (Kgaswane, 2002), in good agreement with the results from receiver functions in the vicinity of the Witwatersrand basin.

8. Regional variations in the deep crust and uppermost mantle

Variations in the thickness of the crust for the Kaapvaal craton and surrounding regions estimated from receiver functions were described by Nguuri et al. (2001), who found much greater thicknesses for the northern region (Fig. 7) compared with those of the southern region of the Kaapvaal craton and the Zimbabwe craton. Useful inferences on the nature of the crust can be made by comparing estimates of crustal thicknesses using Pn or Sn times at individual stations with the results from receiver functions (Kwadiba et al., 2003).

The general features of the Archaean crust and uppermost mantle inferred in the present work are slightly different from those of Durrheim and Green (1992) (35–40 km deep Moho overlain by a crust–mantle transition zone of thickness 1–3 km) below the Witwatersrand basin and those of earlier workers (Willmore et al., 1952; Gane et al., 1956; Hales and Sacks, 1959). There are several reasons for this. The

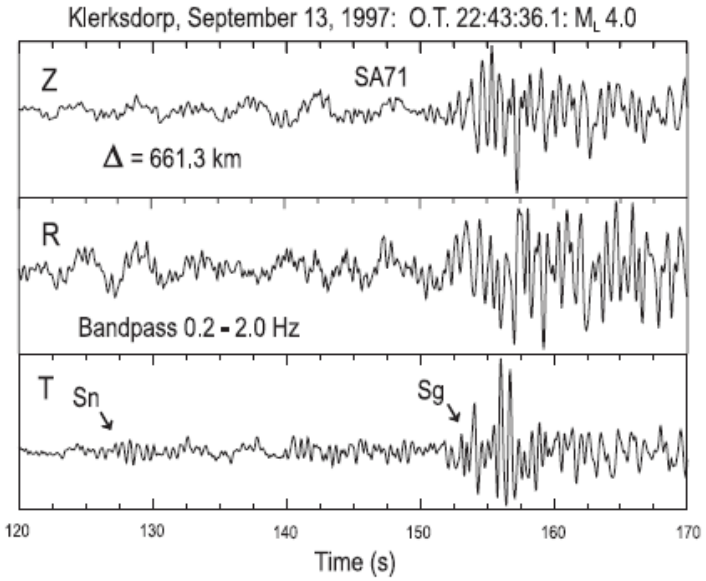

Fig. 14. Seismograms from a mine tremor at Klerksdorp on 13 September 1997 to illustrate observed S phases. Z, R and T denote vertical, radial and tranverse components of motion, respectively. Zero of time scale is from the start of the file, and not from the origin time of the event.

average cross-over distances at which the Pn phase takes over from Pg as the first arrival are now placed at 198–207 and 169–181 km, respectively, for the northern and southern regions, with the lowest and highest values for the Klerksdorp and West Rand regions where the crust below the sources is thinnest and thickest, respectively, (Table 4). Equivalent values, averaged for all three source regions, for the distances at which Sn takes over from Sg are 216 and 188 km, respectively. Previous work by Durrheim and Green (1992) placed the cross-over between Pg and Pn at about 160–170 km for the Witwatersrand basin area (southern part of craton) and suggested an upper mantle wavespeed of 8.1 km/s. The explanation offered for this discrepancy is that the older work did not use arrivals beyond distances of about 300 km, making it difficult to accurately resolve the Pn wavespeeds. An underestimate of the upper mantle wavespeed will also result in crustal thickness estimates that are too low (about 1 km for an error of 0.1 km/s). The present work supports a crustal thickness of 40–43 km and an upper mantle P wavespeed of 8.3–8.4 km/s in the Witwatersrand basin area (Kwadiba et al., 2003).

In the Witwatersrand basin region, seismic reflection profiling shows that the deep crust is no more reflective than the upper crust and there is no identifiable reflection Moho (Durrheim, 1998b), while receiver functions indicate a strong impedance contrast at an average depth of about 38 km. The wavelengths of reflected seismic signals from seismic reflection surveys are around 200–250 m, indicating that large juxtaposed bodies of different compositions due to extensive crustal mixing give rise to relatively weak reflections in the undisturbed regions of the Kaapvaal craton. On the other hand, the wavelengths of the signals that show strong P-to-S conversions (receiver functions) are around 12–15 km. This would require a major change in impedance (bulk composition and/or metamorphic grade) with depth over a depth range of less than about 3 km. This suggests a change from rocks of intermediate composition in the lower crust to highly depleted peridotite over this depth range, with little or no mafic material

sandwiched in between, as proposed by Durrheim and Mooney (1994).

The use of the Pn times to estimate thicknesses of the crust at individual stations is described by Kwadiba et al. (2003), using the assumption of a small bias in origin times to yield minimum crustal thicknesses. If the thickness of the crust in the Witwatersrand basin region is greater than 40 km on the average, the Pn and Sn arrivals imply average crustal thicknesses for 19 stations in the southern region of the craton of 38.07 ± 0.85 km, in agreement with the results from receiver functions, which yield an average of 37.58 ± 0.70 km for the same 19 stations. This is in a region where the P-to-SV conversions in the receiver functions are clear (Fig. 15). These results support the interpretation of the Moho in the southern part of the craton as a relatively sharp transition from rocks of intermediate composition in the lower crust to highly depleted peridotite. However, the average crustal thicknesses inferred from Pn paths to 19 selected northern stations is 50.52 ± 0.88 km, compared with 43.58 ± 0.57 km: some 7 km greater than the average inferred from receiver functions. The greater average crustal thickness determined from refracted arrivals is attributed to the presence of mafic material introduced by underplating. In this northern region, however, receiver functions vary in clarity with estimated thicknesses varying from 38 to 50 km (Fig. 15). How can such differences between two methods of estimating crustal thicknesses be explained by a petrological model of the lower crust?

Hurich et al. (2001) concluded that seismic wavespeed and density in the upper crust, neglecting the effects of open fractures, are dominated by composition. In the middle and lower crust, however, composition and metamorphic grade are equally important. We make use of their conceptual model of continental crust to explain the differences between crustal prop-

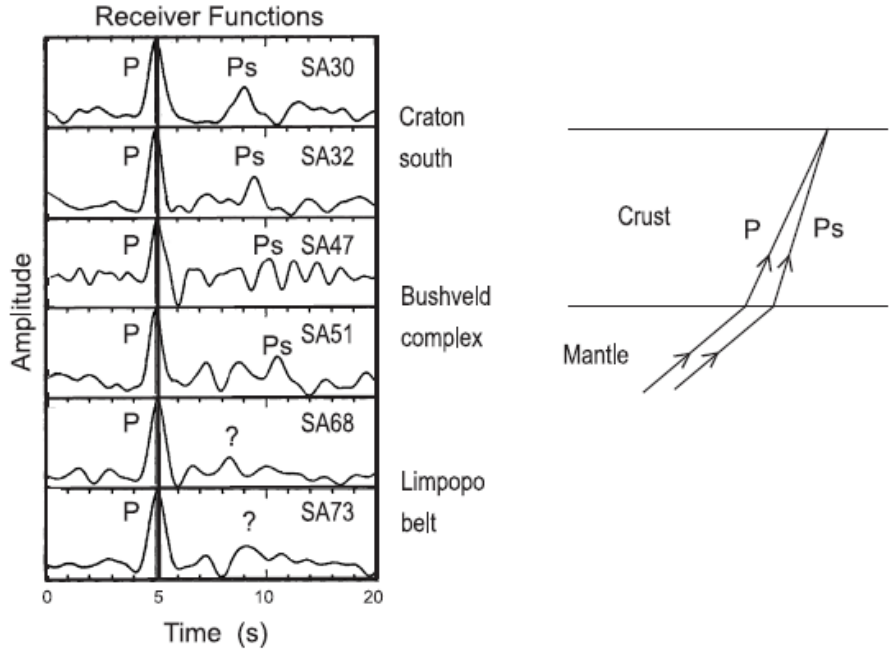

Fig. 15. Examples of receiver functions: stations SA30 and SA32, in the southern part of the Kaapvaal craton, have clear converted S arrivals (Ps); SA47 and SA51, in the Bushveld complex, have complicated receiver functions in which the Ps arrival from the crust–mantle boundary is less clearly defined; SA68 and SA73 lie in the Limpopo belt, where the receiver functions give no clear indication of crustal thickness.

erties for the northern parts of the Kaapvaal craton inferred by receiver functions and refracted arrivals.

Seismic wavespeeds for P and S in the uppermost mantle appear to be similar on the average below the northern and southern parts of the craton. There is also the suggestion that the P wavespeeds are slightly higher in the northern region by about 0.08 km/s (Table 3). The average values for P are in the range 8.3–8.4 km/s, and there is no clear evidence for significant differences in more localised regions (Kwadiba et al., 2003). Such high wavespeeds for Pn indicate that the uppermost mantle consists of a highly depleted, magnesium-rich peridotite across most of the Kaapvaal craton, including the areas affected by the Bushveld magmatism. These values are similar to those obtained for other cratons, particularly the recent values of Langston et al. (2002) for the Tanzanian craton. Most importantly, the processes that resulted in the thick crust beneath the Bushveld complex and much of the remaining northern regions of the Kaapvaal craton clearly had little effect on the peridotites of the uppermost mantle.

Both Hynes and Snyder (1995) and Hurich et al. (2001) have indicated that it is possible for significant portions of the lower continental crust to have wavespeeds indistinguishable from mantle peridotites, provided that the lower crust is almost entirely of mafic composition. This is less likely to occur in Archaean cratons where the wavespeeds of mantle peridotites are very high. Nevertheless, the impedance contrasts between mafic lower crust and peridotitic upper mantle may be so low that appreciable P-to-SV conversion cannot occur. A larger impedance contrast will then occur across the boundary between the mafic lower crust and intermediate middle crust (Table 6; Fig. 16). We suggest that this occurs in parts of the northern and western parts of the Kaapvaal craton, where receiver functions show complexity or variability between nearby stations.

Table 6 shows P wavespeeds, densities and impedances for rock types likely to be found in the middle and lower crust, based on data from Rudnick and Fountain (1995) and Hurich et al. (2001). Because shear-wave data to match those of Hurich et al. are not available, shear wavespeeds were calculated from the P wavespeeds assuming Poisson's ratios of 0.26 and 0.25 for felsic-intermediate and ultramafic rocks, respectively, 0.28 for mafic rocks in the lower crust and 0.27 for eclogites. The values of Poisson's ratio are based on the data compiled by Rudnick and Fountain (1995). All laboratory measurements correspond to room temperature and confining pressures of 400 MPa (Hurich et al., 2001) and 600 MPa (Rudnick and Fountain, 1995). The calculations of impedances are approximate, and no corrections for temperature or pressure have been applied. Wavespeeds of mantle peridotites are those estimated from Pn and Sn data (Table 3).

The amplitudes of P-to-SV conversions will depend most strongly on changes in S wave impedance or S wavespeed, and the effects of changes in P wavespeed are negligible (Appendix A). Fig. 16 shows a simplified, conceptual model for the lower crust of the Kaapvaal craton. The top half of the figure

Table 6
P and S wavespeeds, densities and impedances of rocks that might be found in the deeper parts of the Kaapvaal craton

Rock type	Source of information	P and S wavespeeds (km/s)	Density (kg/m^3)	P wave impedance (kg/(m^2 s))	S wave impedance (kg/(m^2 s))
Granulite facies, intermediate composition	Rudnick and Fountain, 1995; Hurich et al., 2001	6.70, 3.82	2900	19.4×10^6	11.1×10^6
Mafic rocks, upper amphibolite facies	Hurich et al., 2001	7.00, 3.87	3070	22.8×10^6	11.9×10^6
Mafic granulites, plagioclase-rich	Hurich et al., 2001	7.27, 4.02	3190	23.2×10^6	12.8×10^6
Mafic granulites, plagioclase-poor	Hurich et al., 2001	7.60, 4.20	3280	24.9×10^6	13.8×10^6
Mafic rocks in eclogite facies	Rudnick and Fountain, 1995; Hurich et al., 2001	8.00, 4.63	3390	27.1×10^6	15.7×10^6
Kaapvaal peridotites	Durrheim and Mooney, 1994; Table 3	8.20–8.40,[a] 4.84	3200–3300	27.0×10^6	15.7×10^6

[a] P wavespeed estimates are based on data from Table 3, noting that a higher wavespeed is more likely to be associated with iron depletion and therefore a lower density.

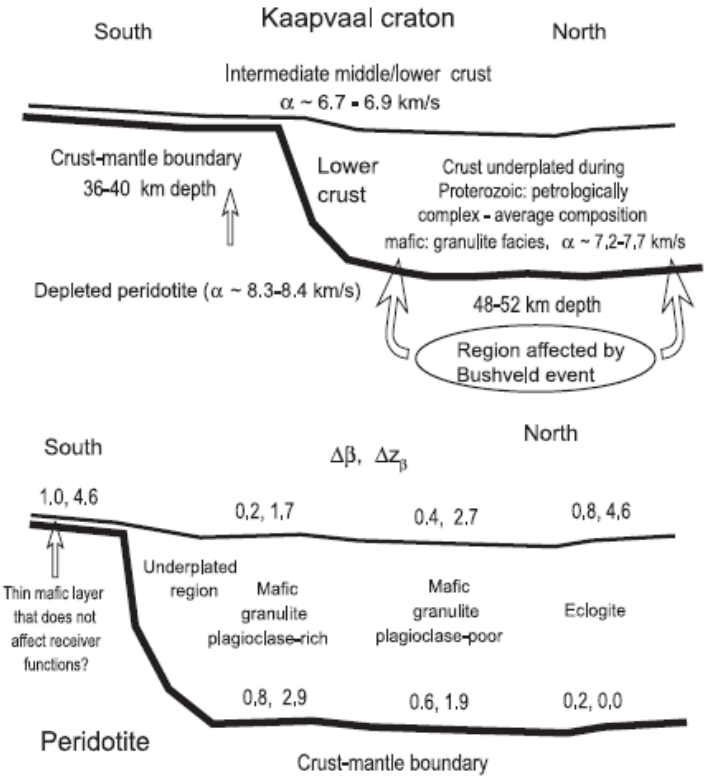

Fig. 16. Schematic model of the lower crust and upper mantle of the Kaapvaal craton (not to scale). $\Delta\beta$ and Δz_β represent changes in shear wavespeed (in km/s) and shear wave impedance with the factor of 10^6 kg/(m^2 s) omitted. The numerical values are from Table 6. The lower section is an expanded representation of the northern region in which the effect of changes in composition and metamorphic grade at the top and bottom of the mafic lower crust are shown. P and S wavespeed are represented by α and β, respectively.

shows the crust–mantle boundary (thick line) in the southern part of the craton between intermediate granulite and depleted peridotite at depths between 36 and 40 km (40–44 km below the Witwatersrand basin). To the north of the boundary marked in Fig. 7, mafic rocks were introduced below the old Archaean Moho, mainly during the Bushveld event, accompanied by intrusion of mafic material (Bushveld complex) into the lower crust in some localities. This mafic material results in a crust–mantle boundary at 48–52 km depth over much of the northern part of the Kaapvaal craton. Because of variations in composition and metamorphic grade across the region, the seismic properties of the lower crust are highly variable, so that receiver functions give no clear indication of crustal thicknesses. This idea is illustrated in the lower half of Fig. 16. In the southern part of the craton, the impedance contrast for S is 4.6×10^6 kg/m^2 s, and the change in S wavespeed is more than 1.0 km/s, giving rise to strong P-to-SV conversions. For the north, three possible situations are shown. If the lower crust is predominantly plagioclase-rich mafic granulite, the impedance and wavespeed contrasts are higher at the crust–mantle boundary than at the top of the lower crust, giving rise to a stronger P-to-SV conversion at the Moho. If, however, the lower crust consists of plagioclase-poor mafic granulites, the stronger conversion will be at the top of the lower crust. In the

extreme case of an eclogitic lower crust, there will be very little P-to-SV conversion at the petrological Moho, and a relatively strong conversion at the boundary between mafic lower crust and intermediate upper crust. The real situation is most likely one of extreme complexity, in which the lower crust is petrologically complex, and contains mafic rocks of variable composition and metamorphic grade. This would give rise to situations when the receiver functions are sometimes dominated by P-to-SV conversions at the Moho, and at other locations by conversions at the top of the mafic lower crust. This phenomenon is proposed as an explanation for the greater crustal thicknesses inferred from Pn and Sn arrivals due to the variable seismic properties of the Moho. The crust–mantle model of Fig. 16, particularly the thicknesses of the underplated and undisturbed regions of the Kaapvaal craton, is also geometrically similar to that of the Archaean Kapuskasing structure (Boland and Ellis, 1989). The estimates of crustal thicknesses for the northern part of the craton will be underestimated, because of the fitting of data to crustal models with a wavespeed of 7.1 km/s at the base of the crust (Table 2); actual values for a mafic lower crust will be significantly higher.

Information from mafic granulite xenoliths that might assist in better understanding the properties of the lower crust is restricted largely to the southern part of the craton (Huang et al., 1995; Dawson et al., 1997). Mafic granulites are rare in kimberlite pipes in the southern part of the craton, but more common in kimberlite pipes of the adjacent mobile belts (Griffin et al., 1979), supporting the model of the Archaean crust/mantle transition of Durrheim and Mooney (1994) in which there is little mafic material in the lower crust.

9. Conclusions

Accurate locations of more than 4400 earthquakes associated with gold mining on the margin of the Witwatersrand basin have been obtained over a 25-month period from specialised seismic networks deployed by the gold-mining industry to monitor seismic activity around deep-mining operations. Most of these events are located with errors of less than 400 m, making them comparable with large explosive sources for the determination of the structure of the crust and uppermost mantle. Errors in locations of events in the mining areas made by the South African network and the Kaapvaal network average about 9.5 and 1.6 km, respectively. Many larger events that were not present in the mine catalogues can therefore be relocated using the Kaapvaal network and used in future studies of earth structure.

The average thickness of the crust below the Kaapvaal craton determined from P and S refracted arrivals from accurately located mining-induced earthquakes is about 47–49 km for paths to the northern and 40–42 km to southern regions of the Kaapvaal craton from sources on the edge of the Witwatersrand basin. If the thickness of the crust is assumed to lie in the range 40–43 km below and around the Witwatersrand basin, as suggested by the results from receiver functions, the average crustal thicknesses determined by the two methods are in good agreement (38 km) for the southern regions of the craton. In these southern regions, where receiver functions imply a sharp crust–mantle boundary, the crust–mantle transition is adequately explained as a boundary between granulites of intermediate composition and a highly depleted peroditite with little or no mafic material in the lowermost crust. The estimated crustal thicknesses around the Witwatersrand basin are also greater by 4–8 km than in previous studies in South Africa that have made use of recordings of mining-induced earthquakes.

The refracted arrivals give an average crustal thickness for the northern parts of the Kaapvaal craton of 51 km, compared with 44 km from receiver functions. The estimated difference in crustal thickness between the two methods for the region that was disturbed by post-Archaean tectonism is attributed to the complexity of the lowermost crust resulting from underplating, particularly during the Proterozoic Bushveld event at 2.05 Ga. Mafic rocks within the lowermost crust can have a wide range of seismic properties that depend on both composition and metamorphic grade. Thus, whenever the lower crust is predominantly mafic, S wavespeed contrasts at the crust–mantle boundary and at the upper boundary of the mafic region, can vary widely from one region to another, causing wide variability in the appearance of receiver functions. In contrast, the Pn or Sn energy

travels within the high wavespeed uppermost mantle, even when the seismic properties of the lower crust approach those of the upper mantle, thereby providing more reliable definition of the petrological crust–mantle boundary.

The uppermost mantle beneath the Kaapvaal craton is remarkably uniform in properties, having relatively high seismic wavespeeds that imply a highly depleted magnesium-rich perodotite. However, the southern boundary of the craton is clearly defined seismically by an increase in crustal thickness and a decrease in upper mantle wavespeed. Changes in seismic character at the northern margin of the craton are less clearly defined.

Acknowledgements

Financial support from the National Research Foundation (South Africa), the National Science Foundation (USA), the University of the Witwatersrand Research Council and from several South African and foreign mining companies who contributed to the running costs and establishment of the Kaapvaal broad-band network is gratefully acknowledged. We also thank members of the Kaapvaal working group from many different organisations in southern Africa and the USA for their assistance. Staff of AngloGold, the Council for Geoscience, East Rand Proprietary Mines, Gold Fields South Africa and ISS International provided valuable sources of information on earth tremors located by the South African network and mine networks, for which we are very grateful. E.M. Kgaswane received financial support from the National Research Foundation and the Council for Geoscience, M.T.O. Kwadiba from the Government of Botswana and the Kellogg Foundation, R.E. Simon from the University of Botswana, and T.K. Nguuri from the Mellon Foundation. The contributions of S.J. Webb to the studies of seismicity are also acknowledged.

Appendix A

At seismic wavespeeds and densities likely to be found in the lowermost crust and uppermost mantle (Table 6), the following results have been derived to illustrate the dependence of P-to-SV conversion amplitudes on changes in impedance, P and S wavespeed, and density. If the average impedances for P and S (products of wavespeed and density), the P and S wavespeeds and densities at the crust–mantle boundary are denoted Z_α, Z_β, α, β and ρ, respectively, and the corresponding changes in these parameters across the crust–mantle boundary ΔZ_α, ΔZ_β, $\Delta\alpha$, $\Delta\beta$ and $\Delta\rho$,

$$\Delta Z_\alpha / Z_\alpha = \Delta\rho/\rho + \Delta\alpha/\alpha \tag{A1}$$

and

$$\Delta Z_\beta / Z_\beta = \Delta\rho/\rho + \Delta\beta/\beta \tag{A2}$$

where

$$\alpha = (\alpha_1 + \alpha_2)/2, \quad \beta = (\beta_1 + \beta_2)/2 \quad \text{and} \quad \rho = (\rho_1 + \rho_2)/2 \tag{A3}$$

$$\Delta\alpha = \alpha_1 - \alpha_2, \quad \Delta\beta = \beta_1 - \beta_2 \quad \text{and} \quad \Delta\rho = \rho_1 - \rho_2 \tag{A4}$$

The subscripts 1 and 2 denote parameter values in the uppermost mantle and lowermost crust, respectively, and Eqs. (A1) and (A2) hold provided the changes in parameters are small.

Suppose α and β are kept constant and the P-to-SV transmission coefficient C is plotted as a function of $\Delta\rho/\rho$, for a boundary between ultramafic and mafic rocks, and for a P wave arrival of apparent wavespeed of 16.0 km/s, corresponding to a shallow earthquake at a distance of about 59°. The slope of the graph is almost constant at 0.10 over a range of $\Delta\rho/\rho$ values of about 0.1. Similarly, if α and ρ are kept constant, the slope of the plot of C against $\Delta\beta/\beta$ is almost constant at 0.51. Finally, when β and ρ are kept constant, the slope of the plot of C against $\Delta\alpha/\alpha$ is 0.039.

Thus, C depends most strongly on the change in S wavespeed, with the change in density providing a smaller but significant dependance. The change in P wavespeed has only a slight effect on C. C therefore depends on ΔZ_α through the density change only, whereas the dependence on ΔZ_β involves both changes in S wavespeed and density, but with a fractional change in β having about five times the effect of a similar change in ρ (Eqs. (A1) and (A2)).

All calculations have been undertaken using the Zoeppritz equations listed on page 150 of Aki and Richards (1980). It is also noteworthy that over the teleseismic distance range (30–95°), C decreases by a factor of about 2 due to the decrease in angle of incidence of the P wave at the crust–mantle boundary.

References

Aki, K., Richards, P.G., 1980. Quantitative Seismology, Theory and Methods, vol. 1. Freeman, San Francisco. 557 pp.

Andreoli, M.A.G., Doucouré, M., Van Bever Donker, J., Brandt, D., Andersen, N.J.B., 1996. Neotectonics of southern Africa—a review. Afr. Geosci. Rev. 3, 1–16.

Boland, A.V., Ellis, R.M., 1989. Velocity structure of the Kapuskasing Uplift, Northern Ontario, from seismic refraction studies. J. Geophys. Res. 94, 7189–7204.

Bolt, B.A., 1978. Summary value smoothing of physical time series with unequal intervals. J. Comput. Phys. 29, 357–369.

Carlson, R.W., Grove, T.L., de Wit, M.J., Gurney, J.J., 1996. Program to study crust and mantle of the Archean craton in southern Africa. Eos Trans. Am. Geophys. Union 77 (29), 273 and 277.

Dawson, J.B., Harley, S.C., Rudnick, R.L., Ireland, T.L., 1997. Equilibration and reaction in Archaean quartz–sapphirine granulite xenoliths from the Lace kimberlite pipe, South Africa. J. Metamorph. Petrol. 15, 253–266.

Durrheim, R.J., 1998a. Seismic refraction investigations of the Kaapvaal craton. S. Afr. Geophys. Rev. 2, 29–35.

Durrheim, R.J., 1998b. A deep seismic reflection profile across the Witwatersrand basin. S. Afr. Geophys. Rev. 2, 69–73.

Durrheim, R.J., Green, R.W.E., 1992. A seismic refraction investigation of the Archaean Kaapvaal Craton, South Africa, using mine tremors as the energy source. Geophys. J. Int. 108, 812–832.

Durrheim, R.J., Mooney, W.D., 1994. Evolution of the Precambrian lithosphere: seismological and geochemical constraints. J. Geophys. Res. 99, 15359–15374.

Gane, P.G., Hales, A.L., Oliver, H.O., 1946. A seismic investigation of the Witwatersrand earth tremors. Bull. Seismol. Soc. Am. 36, 49–80.

Gane, P.G., Atkins, A.R., Sellschop, J.P.F., Seligman, P., 1956. Crustal structure in the Transvaal. Bull. Seismol. Soc. Am. 46, 293–316.

Graham, G. (Ed.), 1997. Seismological Bulletins (produced monthly). Council for Geoscience, Pretoria, South Africa, April–December issues.

Graham, G. (Ed.), 1998. Seismological Bulletins (produced quarterly). Council for Geoscience, Pretoria, South Africa, January–March, April–June, July–September and October–December issues.

Graham, G. (Ed.), 1999. Seismological Bulletins (produced quarterly). Council for Geoscience, Pretoria, South Africa, January–March and April–June issues.

Green, R.W.E., Bloch, S., 1971. The Ceres, South Africa, earthquake of September 29, 1969. Bull. Seismol. Soc. Am. 61, 851–859.

Green, R.W.E., Chetty, P., 1990. Seismic studies in the basement of the Vredefort structure. Tectonophysics 171, 105–113.

Griffin, W.L., Carswell, D.A., Nixon, P.H., 1979. Lower crust granulites and eclogites from Lesotho, southern Africa. In: Boyd, F.R., Meyer, H.O.R. (Eds.), The Mantle Sample: Inclusions from Kimberlites and Other Volcanics. American Geophysical Union, Washington, pp. 59–86.

Hales, A.L., Sacks, I.S., 1959. Evidence for an intermediate layer from crustal structure studies in the Eastern Transvaal. Geophys. J. R. Astron. Soc. 2, 15–33.

Huang, Y.-M., Van Calsteren, P., Hawkesworth, C.J., 1995. The evolution of the lithosphere in southern Africa: a perspective on the basic granulite xenoliths from kimberlites in South Africa. Geochim. Cosmochim. Acta 59, 4905–4920.

Hurich, C.A., Deemer, S.J., Indares, A., 2001. Compositional and metamorphic controls on velocity and reflectivity in the continental crust: an example from the Grenville Province of eastern Québec. J. Geophys. Res. 106, 665–682.

Hynes, A., Snyder, D.B., 1995. Deep crustal mineral assemblages and potential for crustal rocks below the Moho in the Scottish Caledonides. Geophys. J. Int., 323–339.

Jeffreys, H., 1937. On the smoothing of observed data. Proc. Camb. Philos. Soc. 33, 444–450.

Kgaswane, E.M., 2002. The Characterisation of Natural and Human-Related Seismicity in Southern Africa: April 1997–April 1999. MSc dissertation, University of the Witwatersrand, Johannesburg, 110 pp.

Kgaswane, E.M., Wright, C., Kwadiba, M.T.O., Webb, S.J., McRae-Samuel, R., 2002. A new look at South African seismicity using a temporary network of seismometers. S. Afr. J. Sci. 98, 377–384.

Kwadiba, M.T.O., Wright, C., Kgaswane, E.M., Simon, R.E., Nguuri, T.K., 2003. *Pn* arrivals and lateral variations of Moho geometry beneath the Kaapvaal craton. Lithos 71, 393–411 (this issue).

Lahr, J.C., 1989. HYPOELLIPSE/Version 2.0: a computer program for determining local earthquake hypocentral parameters, magnitudes and first motion patterns. U.S. Geological Survey Open-File Report 89-116, 92 pp.

Langston, C.A., Nyblade, A.A., Owens, T.J., 2002. Regional wave propagation in Tanzania, East Africa. J. Geophys. Res. 107 (B1), 1–18 (ESE1).

Mendecki, A.J. (Ed.), 1997. Seismic Monitoring in Mines. Chapman & Hall, London. 262 pp.

Nguuri, T.K., Gore, J., James, D.E., Webb, S.J., Wright, C., Zengeni, T.G., Gwavava, O., Snoke, J.A.Kaapvaal Seismic Group, 2001. Crustal structure beneath southern Africa and its implications for the formation and evolution of the Kaapvaal and Zimbabwe cratons. Geophys. Res. Lett. 28, 2501–2504.

Reinsch, C.H., 1967. Smoothing by spline functions. Numer. Math. 19, 177–183.

Richards-Dinger, K.B., Shearer, P.M., 1997. Estimating crustal thickness in southern California by stacking PmP arrivals. J. Geophys. Res. 102, 15211–15224.

Rudnick, R.L., Fountain, D.W., 1995. Nature and composition of the continental crust: a lower crustal perspective. Rev. Geophys., 267–309.

Shearer, P.M., 1999. Introduction to Seismology. Cambridge Univ. Press, Cambridge, UK. 260 pp.

Simon, R.E., Wright, C., Kgaswane, E.M., Kwadiba, M.T.O., 2002. The P wavespeed structure below and around the Kaapvaal craton to depths of 800 km, from travel times and waveforms of local and regional earthquakes and mining-induced tremors. Geophys. J. Int. 151, 132–145.

Simon, R.E., Wright, C., Kwadiba, M.T.O., Kgaswane, E.M., 2003. Mantle structure and composition to 800-km depth beneath southern Africa and surrounding oceans from broadband body waves. Lithos 71, 353–367 (this issue).

Webb, S.J., Wright, C., Kgaswane, E.M., 2001. Characterization of natural and human-related seismicity in South Africa: April 1997 to April 1999. Report (with database) sponsored by U.S. Defense Special Weapons Agency (principal investigator, T.H. Jordan, University of Southern California).

Willmore, P.L., Hales, A.L., Gane, P.G., 1952. A seismic investigation of crustal structure in the western Transvaal. Bull. Seismol. Soc. Am. 42, 53–80.

Wood, H.E., 1913. On the occurrence of earthquakes in South Africa. Bull. Seismol. Soc. Am. 3, 113–120.

Wright, C., Kwadiba, M.T.O., Kgaswane, E.M., Simon, R.E., 2002. The structure of the crust and upper mantle to depths of 320 km beneath the Kaapvaal craton, from P wave arrivals generated by regional earthquakes and mining-induced tremors. J. Afr. Earth Sci. 35, 477–488.